Journal of Metals, Materials and Minerals, 33(3), 1709, 2023

The changes in microstructural features and physical properties of ceramic matrix composite bonding tools under ultrasonic service

Apirat THEERAPAPVISETPONG [1,2] , Karn SERIVALSATIT [1,2], Wuttichai REAINTHIPPAYASAKUL[1,2], and Wantanee BUGGAKUPTA[1,2,*]

[1] *Department of Materials Science, Faculty of Science, Chulalongkorn University, 254 Phayathai Road, Pathumwan, Bangkok, 10330, Thailand*
[2] *Center of Excellence on Petrochemical and Materials Technology, Chulalongkorn University, 254 Chulalongkorn 12 Street, Phayathai Road, Pathumwan, Bangkok, 10330, Thailand*

***Corresponding author e-mail:** Wantanee.b@chula.ac.th

Received date:
11 April 2023
Revised date
11 August 2023
Accepted date:
15 August 2023

Keywords:
Ultrasonic bonding;
Bonding tool;
Microstructures;
Characterization

Abstract

Tape automated bonding (TAB) process plays a key role in the production of disk drives, microchips and other microelectronics components. Such tools should sustain their structures and properties throughout ultrasonic operation and are expected to last until reaching the targeted numbers of TAB cycles. This project aims to evaluate the changes in microstructures and physical properties of the bonding tools under ultrasonic service. Three commercial waffle-type tools from different suppliers were focused, namely Tool A, Tool B and Tool C. They provide different levels of bonding efficiency up to 50k cycles under relatively similar ultrasonic practice. Non-destructive and destructive testing methods were examined by the means of X-Ray and mass spectroscopy techniques, respectively. The waffle-end tips of the selected tool were observed using a confocal microscope. The changes in grain size and grain size distribution before and after ultrasonic service were quantitatively analyzed via electron micrographs. Also, their bulk density, hardness and toughness were determined. The experimental work revealed the variation in microstructural features and properties among the three, leading to the difference in ultrasonic efficiency, even they all contained similar phase composition. The relationship between microstructures, properties and ultrasonic efficiency was also reported and discussed.

1. Introduction

Ultrasonic bonding is one of the most practical wire bonding techniques for electrical interconnection in microelectronic components. The ultrasonic bonding process involves the generation of inter-connectivity between circuitry of the die to the external surrounding via a wire with the help of force, applied power, time, ultrasonic vibration and temperature, in some cases. The wire bonding can be categorized as thermocompression (heat and force), thermosonic (heat and vibration) and ultrasonic actions [1-3]. Ultrasonic vibrational energy was initially introduced in the year of 1960s, commonly known as ultrasonic energy or acoustic wave. Ultrasonic energy is a form of mechanical energy generated from sound and characterized by a vibration of particles within a medium with a frequency greater than 20000 Hertz (20 kHz) which is above the audible sound range frequency (20 Hz to 20000 Hz). Ultrasonic energy is produced from an ultrasonic transducer, converting the electrical energy to the mechanical one. The ultrasonic energy requires a matter or a medium with particles to oscillate in order to conduct or propagate its energy. Assuming a particle and its neighbouring particles are in equilibrium and they are under interatomic force. The energy travels through most medium in the form of wave due to the displaced or deformed particles according to vibration under elastic service [4,5]. Ultrasonic action benefits the wire bonding in the term of its low temperature. The bonding operation at ambient temperature induces bonding reliability, bond strength and prevents both wire and substrate natures at the interfacial contact from oxidation. New generation of advanced electronic packages with compact, high performance, low power consumption, functional but high reliability and also low cost, has driven the bonding technology to go far beyond its limitations. The key factors include ultrasonic behavior, knowledge of bonding operation and proper bonding tool selection.

A solid phase welding which uses a thin wire and a combination of force and ultrasonic power, the equipment setup and special bonding tool are crucially required. The setup comprises a piezoelectric transducer that generates vibrational energy which attached to a horn or the tool holder. The horn clamps the tool tightly. Ultrasound wave propagates as a longitudinal wave along the horn and then converts to transverse wave in the bonding tool. Bonding tools play their roles as a medium, allowing the energy to travel through in the form of wave that is likely to travel and propagate in a bonding media in transverse manners [4]. Therefore, the tangential displacement oscillates at the tip of the tool, transferring the energy through the wire and the substrate to be bonded. As far as the bonding tools are considered, there are three main bonding tool types according to their geometries and bonding characteristics: capillary (ball bonding),

wedge bonding and single-point TAB (tape automated bonding) tools. Even though capillary bonding is a worldwide bonding technique applied in microelectronic industries, it has several drawbacks, e.g. poor deep access, lifted ball and stitch, as mentioned elsewhere [1,2,4]. Later on, the wedge bonding has been developed in order to solve such drawbacks. Both capillary bonding and wedge bonding have similar bonding manners, i.e. a wire has to be threaded through the tool, which limits rotational motion during bonding service, resulting in unstable and slow bonding rate. To reduce unstable force and consequence strength of the bonded leads, a method of bonding each lead separated was developed, so called single-point tab bonding (a single-point TAB). A single-point TAB commonly refers to a lead, trace, wire or ribbon that one-side of which is already in position and needs to be automatically bonded using a coupling of force and ultrasonic energy [6-8]. More flexible tip design and configuration of the TAB tool are possible which can improve pull strength, bonding rate as well as bonding efficiency. Such patterns offer more aggressive impression and offer better ultrasonic energy transmittance.

Bonding quality strongly depends on tip finish, physical and chemical properties, mechanical bonding and ultrasonic performance. As far as the ultrasonic bonding tools are concerned, the selection of the proper materials, preparation of the material feedstocks to the right manufacturing processes using the right equipment and techniques to sustain flexibility, dimensional precision with qualified properties are of importance. The tools used for ultrasonic applications are considered consumable, thus, tool materials should provide mechanical durability, hardness to prevent deformation, high stiffness and abrasive resistance. Also, electrostatic discharge that can damage the components is to be prevented. Ceramic materials meet such requirements and also favour several impressive benefits to ultrasonic bonding activities. Ceramic-based tools are applicable to a variety of wires: gold wires, copper wires, aluminum wires, or gold ribbons. So, ceramic materials undoubtedly become the best option.

Ceramic bonding tools require high precision processing technology, configuration design and manufacturing production to fit bonding natures, bond materials and pad characteristics. Longer service life and high wear resistance has been accomplished by the right raw materials. For the ceramic bonding tools, zirconia (ZrO_2), zirconia toughened alumina (ZTA), or alumina-zirconia (Al_2O_3-ZrO_2) composites are commonly employed due to their superior mechanical and physical properties comparable to the standard plain Al_2O_3. Furthermore, raw materials for ceramic bonding tools cover tungsten carbide (WC), titanium carbide (TiC), even cermet [2,9]. In some cases, a surface coating is also accommodated using a diamond-like carbon (DLC) in order to extend the tool life span.

As mentioned above, tool materials developed from stabilized ZrO_2, ZTA or Al_2O_3-ZrO_2 composites are most commonly used in ultrasonic applications. The addition of chromium oxide (Cr_2O_3) is introduced in the microstructure in order to improve hardness and claimed more or less to induce ultrasonic efficiency, higher density and reduced grain sizes [1,2]. It can be noticeably seen from its colours: pink and purple shades. Some reviews [e.g. 1-3,9] suggested that the small amount of Cr_2O_3 in ZTA and achieves the highest hardness and bending strength values than that of the standard ceramic (pure Al_2O_3). Ma and Zhao [10] focused on the effects of ultrasonic frequencies on both of cyclic amplitude and fatigue life of Al_2O_3-ZrO_2 nanocomposite ceramics. The results showed that during the low load level tests, fracture toughness was induced by the transcrystalline (transgranular) fracture showing the existence of the inhibition effect on the crack initiation and propagation. Additionally, tetragonal (t) -monoclinic (m) phase transition of ZrO_2 under higher frequency (approximately 30 kHz) was observed. Cyclic amplitude and the fatigue life can be improved with increasing ultrasonic frequency. High frequencies could exhibit stronger toughening improvements than the lower ones did. However, it is noticed that microstructural features and properties of the commercial Al_2O_3-ZrO_2 bonding tools always vary with its chemical composition [1,9]. Boniecki *et al*. [11] reported the variation in density, average grain size as well as Weibull strength distribution. Finer grain of Al_2O_3 matrix, higher density values and strength were achieved with higher contents of ZrO_2. Some studies [12,13] found that ultrasonic velocity through Al_2O_3-ZrO_2 ceramic composite bodies was faster in a medium with high Al_2O_3 content. However, the studies in microstructure and properties Al_2O_3-ZrO_2 ceramic composite as a result of ultrasonic application are very few.

Practically, the utilization of ceramic bonding tools in industrialized ultrasonic service is targeted by the number of bonding cycles or TAB cycles. This work stated the industrial-based problems upon Al_2O_3-ZrO_2 composite under ultrasonic service. A waffle-type TAB tool was of interests. When one bonding tool the performance of which was excellent in the production line and met most bonding requirements were discontinued or no longer produced, other new candidate tools were to be replaced. Claimed that the characteristics were desirable by the tool suppliers, however, the user later discovered that the replaced tools were not as good as the previous one, under relatively similar bonding practice. Service life of the tool were shorter than the targeted TAB cycles and bonding quality was unsatisfactory. Thus, our research work is to sort out what are the causes of the problems based on tool characterization. Our assumptions cover the relationship between microstructural features, composition, material properties and bonding efficiency. The variation of these factors before and after ultrasonic service of the selected bonding tools are to be both qualitatively and quantitatively analyzed. A series of bonding tools from 3 different manufacturers collected the user's from production line were characterized, compared, reported, and discussed.

2. Experimental

Three commercial waffle-type bonding tools from different manufacturers were concerned, designated as Tool A, Tool B and Tool C. A series of the new and the used bonding tool samples were collected. The used ones underwent different levels of bonding cycles (up to 50k) under relatively similar ultrasonic practice. The end-of-use tool samples were collected after being employed at different cycles because some might fail, deform or give disqualified stitch or bond foot. Both non-destructive testing (NDT) and destructive testing (DT) methods were conducted, respectively. The as-received bonding tools were thoroughly cleaned. The density measurement was done by a de-aired liquid immersion method. The tool dimensions were measured and the waffle-tips of the bonding tools were observed

using a confocal microscope and a scanning electron microscope. Phase presence and chemical composition of the tips was examined by the means of X-ray diffractometry (XRD) and energy dispersive spectroscopy (EDS) techniques. After NDT, the tool samples were undergone grinding and polishing, Vickers hardness (HV) and fracture toughness (K_{IC}) values were obtained by an indentation method using the load of 10 kg (98.1 N). The hardness values of the tool samples were calculated from Equation 1 while fracture toughness values were obtained from average diagonals ($\bar{d}$) along with average crack length ($\bar{C}$) of the indented marks. The marks presented onto the polished surfaces were considered as Median cracks and were estimated using the equation conducted by Tanaka model [14,15] as shown in equation 2, that is:

$$HV = 1.8544 \frac{P}{\bar{d}^2} \quad (1)$$

$$K_{IC} = 0.0752 \frac{P}{\bar{C}^{3/2}} \quad (2)$$

After that, the samples were thermally etched at 1500°C for 5 min in air, followed by the microstructural observation using an electron microscope. Grain size and grain size distribution information were collected via backscattered electron micrographs and evaluated with the help of ImageJ software [16]. Finally, the bonding tool samples were crushed into powders to prepare subsamples. Each tool subsample was dissolved in a mixture of lithium metaborate ($LiBO_2$) and lithium bromide (LiBr) at the temperature of 1200°C, then a flux solution containing a mixture of nitric acid (32 %w/v) and hydrochloric acid (17.5 %w/v) was added until all melt dissolved. The derived fluid solution after digestion was ready to be chemically analyzed by the mean of an induced coupled plasma mass spectroscopy (ICP-MS). Also, the operation details on bonding practice were interviewed and gathered from the user.

3. Results and discussion

According to the tool user, Tool A provided the most desirable functions and properties as targeted. Most of Tool A achieved targeted service life up to 50k cycles and offered bonding ability together with desirable bond foot with minimum tool or bonding failure during service. Thus, Tool A is defined as the benchmark. Other candidate tools (Tool B and Tool C) therefore were expected to have similar bonding performance towards Tool A. Bonding efficiency not only depends on bonding parameters (applied force, power and time of exposure) but also strongly relies on the tool material characteristics. The summarized characteristics and properties of the three tips: Tool A, Tool B and Tool C, are presented in Table 1. The geometries of them were similar, i.e. the waffle-end tips with the length of 11 mm and 1.6 mm in diameter, approximately. The distances between apex of diamonds along the test lines and the height were slightly different. Tool B was 8.5 µm high, followed by Tool A (7 □m) and Tool C (6.5 □m), respectively. The point end of the tool was similar to a plateau representing a flat face along with steep sides, technically so called MESA. The term "MESA" literally means a tableland or a plateau representing an isolated flat-topped with steep side manners. To differentiate from the "geological mesa", this technical term is always written in capital letters, MESA, in the microchip bonding application as seen from many document and literature reviews. Thus the term MESA does not have full name and is not an abbreviation. The differences in MESA area of these tools evaluated from the micrographs were relatively small. The number of diamonds per MESA area (at which diamonds situate and seen as the waffle-end) of Tool C yielded 169 while the other two were 196. It seemed like their geometries and surface profiles of the three tools were very slightly and seemed insignificantly different, as shown in Figure 1 and Figure 2. But in the sense of ultrasonic energy transfer, this could lead to different levels ultrasonic transfer efficiency [1]. Surface finish of the bonding tools comes with different purposes. In case of the capillary tools, the matte finish or rough surface could maximize ultrasonic transfer and enhance mechanical coupling between the bond materials but this was susceptible of the build-up comparatively to the polished one. Thus, the waffle-end configuration of the TAB bonding tools is deliberately designed to maximize surface area where the ultrasonic can transfer through. Unfortunately, it was not very easy to estimate the exact total surface area of the waffle-end tips due to the fact that the sizes, density of the diamonds per area and the distances between diamonds were to be taken into account. It was noticed that the diamond details of each tool was significant different in the term of roughness and neatness, as seen in Figure 1. Tool A presented dense, sharp-edge, square frustum-shaped diamonds. Meanwhile, diamonds presented in Toll B and Tool C contained surface imperfections in some extent. The surface of Tool C was relatively smoother than that of Tool B but Tool C still contained pores at the sharp edges. Tool B surface was quite rough and not very neat. This might come from different fabrication processes. The manufacturing history of Tool B was fabricated by ceramic injection moulding [2] but that of the other two were not technically stated by the tool manufacturers. Starting particle size of raw materials, feedstock preparation, moulding details, injecting temperature and pressure, debinding procedure and thermal history of the tools, however, was not clearly mentioned by the tool manufacturers because such details could truly reveal the secret-trade of their products. The state problem of this work, at the first hand, is to improve the properties of the alternative tool in order that the candidate tools could possibly be improved in some ways. Also, the candidate ones were expected to run smoothly instead of the discontinued benchmark, Tool A, in the production line without or with minimum process reset. The user discovered that the specification of the candidate tools the properties of which were guaranteed by the later manufacturers might not be very precise and did not meet some bonding requirements. Lots of problems were always monitored and the failed bonds were rejected even all candidate tools were under the same bonding service compared with Tool A.

Figure 1 and Figure 2 also revealed shapes and sizes of the end-of-service tools, showing that worn surfaces of the diamonds and the waffle-ends that were not very uniform all over the tip areas. In Tool A, the evidence of the worn diamonds could be noticed and the wear-off section still remained square-shaped, no pores within the internal diamond and no cracks along the edges. Unlike Tool A, Tool B showed uneven wear-off, it could not sustain its frustum-shaped and the wear-off section was not so sharp. Tool C could retain its shapes but the worn surface was severely damaged, suggesting

that Tool C could not withstand wear during ultrasonic service. To evaluate the wear loss, the changes in height profiles after the certain numbers of TAB cycles in Figure 2 pointed out that the relative wear loss per cycle of Tool C ranked highest, in agreement with Figure 1, and performed the lowest wear resistance.

On a basis of ceramic science and some the evidence from bonding tip characterization, these microstructural features could be only obtained from ultrafine raw material powders. The fine particulate mixtures are mixed with some binder(s) and preformed by a process of powder injection moulding. No information about the tool production, i.e. starting particle size of raw materials, feedstock preparation, injecting temperature and pressure, debinding procedure and sintering processes of the tools, was mentioned in any documents or references from the tip manufacturers. What the researcher could investigate was only from their microstructure and properties of the derived tools under the same bonding service. Fortunately, our characterization from the new and the used tools gave us some clues. Finer grain size in Tool A compared with Tool B and Tool C suggested that Tool A was made from finer starting powder raw materials or lower sintering temperature due to its severe grain growth after thermal etching, that would be shown later on. Chemical analysis showed that the starting materials were mainly Al_2O_3 and ZrO_2 powders but various Al_2O_3 and ZrO_2 contents were not the same among these tools. Microstructural features did not strongly affect physical properties but significantly on ultrasonic transfer and wear loss which crucially depends on ultrasonic bonding parameters.

Table 1. Summary of the bonding tool characterization.

Properties	Tool A	Tool B	Tool C
Dimension			
Diameter (mm)	1.6	1.6	1.6
Length (mm)	11.13	11.06	11.13
Distance between diamonds (□m)	7	8.5	6.5
MESA area (□m^2)	87705	89071	73913
No. of diamonds on MESA	196	196	169
Chemical composition (via ICP-MS)			
Phase presence	Al_2O_3 , ZrO_2	Al_2O_3 , ZrO_2	Al_2O_3 , ZrO_2
Phase ratio (ZrO_2: Al_2O_3 mole ratio)	0.786:1	0.205:1	0.123:1
Grain size (□m), new tool			
Alumina (Al_2O_3)	0.47 ± 0.16	0.74 ± 0.28	0.77 ± 0.36
Zirconia (ZrO_2)	0.38 ± 0.10	0.30 ± 0.09	0.34 ± 0.11
Density ($g \cdot cm^{-3}$)	4.45 ± 0.19 (92%TD)	3.69 ± 0.41 (85%TD)	4.22 ± 0.27 (99%TD)
Vickers hardness (HV or $kg \cdot mm^{-2}$)	1709 ± 81	1848 ± 170	1782 ± 168
Fracture toughness ($MPa \cdot m^{-1/2}$)	4.42 ± 0.37	4.87 ± 0.45	3.56 ± 0.06
Relative wear loss (×10^{-5} □m/cycles)	1.26	1.40	1.94

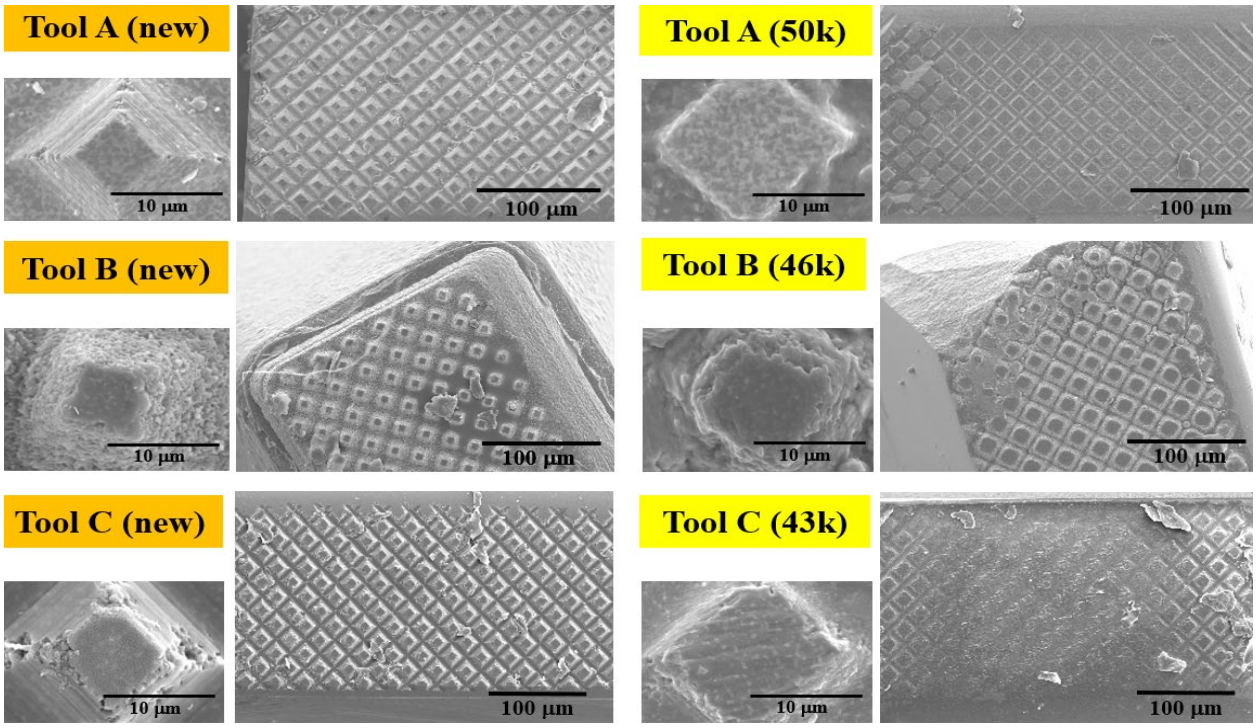

Figure 1. Electron micrographs of the waffle-tip surfaces before and after ultrasonic activities.

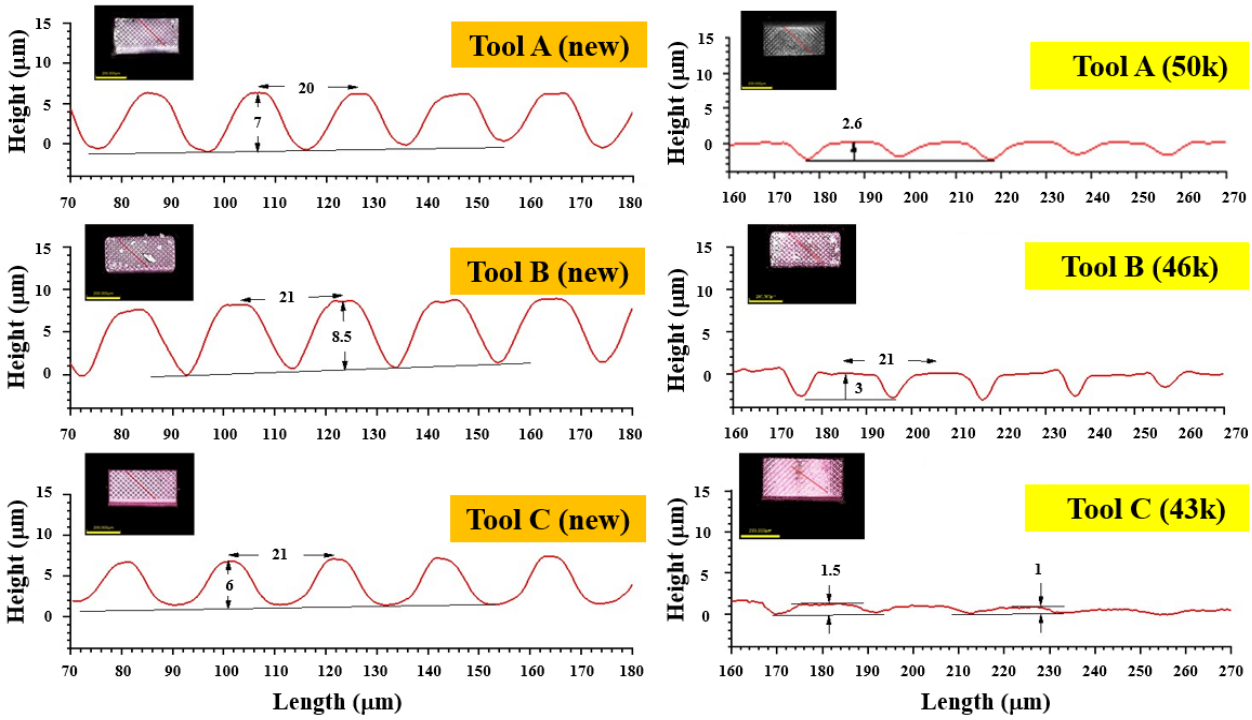

Figure 2. Linear MESA profiles and changes in diamond heights of the bonding tools.

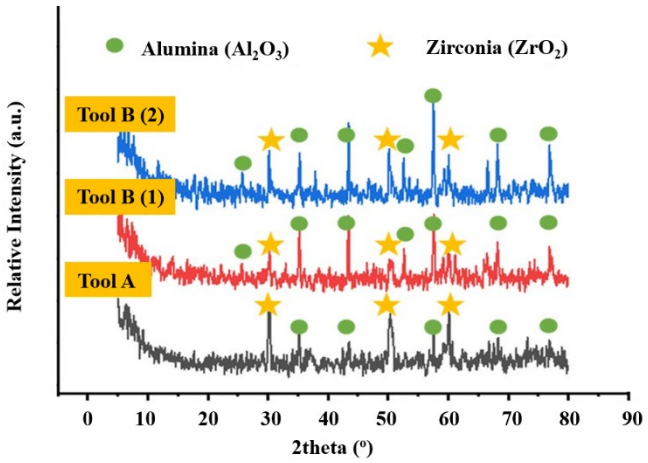

Figure 3. XRD patterns of the as-received tool samples.

It could be observed from the backscattered electron micrographs shown in Figure 1 that the diamonds of all tools comprised of two different phases. The phase content was confirmed by XRD patterns in Figure 3, alumina (Al_2O_3) and tetragonal zirconia (t-ZrO_2) phases were detected. The first three strong peaks of Al_2O_3 presented at 2□□ of 43.8□, 35.0□ and 57.4□ at the planes of (113) (104) and (116), respectively. Meanwhile, t-ZrO_2 presence was confirmed by the peaks at 2□□ of 30.1□, 50.4□ and 60.2□□at the planes of (112) (211) and (101), respectively. From the elemental mapping and EDS area scans in Figure 4 and Table 2, the elements of aluminium (Al), zirconium (Zr) and oxygen (O) could identified as the main constituent elements, representing in blue, green and yellow, respectively. The normalized elemental analysis in Table 2 suggested that all tools were Al_2O_3-based materials reinforced by ZrO_2 but they contained different Al-Zr-O elemental fractions. They all came along with a small amount of chromium (Cr), as shown in pink. The chemical compositions of the tool samples were also quantitatively analyzed using ICP-MS. Focusing only on main phases, the phase ratios are reported in the term of ZrO_2:Al_2O_3 mole ratio, as reported in Table 1. The ratio values of Tool A, Tool B and Tool C were 0.786, 0.205 and 0.123 to 1, respectively, confirming that Tool A microstructure was comparatively ZrO_2-rich. So, the hardness of Tool A was supposed to be lowest among the three tools because hardness of a ceramic body strongly depended on Al_2O_3 content [12]. Regardless any flaws presented in the bodies, the highest hardness values could be expected from Tool C, followed by Tool B, less wear loss might be expected compared with Tool A. However, the existence of ZrO_2 could enhance fracture toughness by toughening and strengthening Al_2O_3-based bodies [11], so called ZTA. ZrO_2 generally toughens Al_2O_3 via two main mechanisms: the grain refinement and martensitic phase transformation [11-13,17]. Ultrasonic energy with high frequency travelling throughout the medium incorporates with ultrasonic stress accumulated in the structure and can induce phase transformation. Several literatures reported the effects of ultrasonic energy coupling other actions, e.g. mechanical, thermal or thermo-mechanical stress, on phase transition in alloys containing unstabilized or partially stabilized phase. Some studies [13] focusing on the evaluation of elastic modulus of Al_2O_3-ZrO_2 composites by ultrasonic waves reported that the ultrasonic transmission could possibly more or less develop shear strain in the bodies, particularly in unstabilized ZrO_2. The deformation-induced martensitic transformation of ZrO_2 from tetragonal to monoclinic phase could somewhat occur even at ambient temperature. In this application, the ultrasonic service runs at room temperature to avoid deterioration of the bond materials. Stress build up comes from 2 sources: applied stress and ultrasonic stress. Ultrasonic energy with high frequency travelling throughout the medium incorporates with ultrasonic stress accumulated in the structure and can induce phase transformation. Some literatures reported the effects of ultrasonic

energy coupling other actions, e.g. mechanical, thermal or thermo-mechanical stress, on phase transition in alloys containing unstabilized or partially stabilized phase. Ceramic materials seem to be much less sensitive to ultrasonic field compared to metal alloys. However, this behaviour was also observed [12,13], the non-destructive testing (NDT) for elastic modulus of Al_2O_3-ZrO_2 composites using ultrasonic waves were conducted. They reported that the ultrasonic transmission could possibly more or less develop shear strain in the bodies, particularly in the unstabilized ZrO_2 –bearing structures. However, these experiments did run ultrasonic transfer neither coupling with a loading pressure nor a long and continuous ultrasonic exposure as the bonding tool practice. Thus, the deformation-induced martensitic transformation of ZrO_2 from tetragonal to monoclinic phase could somewhat occur even at ambient temperature, especially at the tip/bond material interfacial contact where bonding activity took places.

A series of backscattered electron micrographs in Figure 5 reveals the thermally etched microstructural features of the tools. As far as the new tools were considered, it could be clearly seen the areas of the dark field and the light field, representing Al_2O_3 and ZrO_2 grains, respectively. ZrO_2 grains in these new tools looked quite the same size but Al_2O_3 grains in Tool A were much finer than those of Tool B and Tool C. From these microstructural features, it could be expected that Tool A would offer high elastic modulus, strength and toughness whereas Tool B and Tool C provided higher hardness according to different ZrO_2 and Al_2O_3 phase fractions. Fine and uniform grain structures favour superior mechanical properties when strength is required. As far as the grain growth is concerned, grain size could be generally coarsened by 2 main causes: (1) prolonged heat exposure and (2) high sintering temperature. The foreign particles added into the mixture, ZrO_2 in the case, can control grain coarsening via particle pinning. This grain coarsening control in Al_2O_3 by ZrO_2 relating to ultrasonic waves was reported elsewhere [12,13]. According grain size measurement, ZrO_2 grains presented in these tool samples was approximately similar in size, 0.3 □m to 0.4 □m while those of Al_2O_3 matrix were varied (see Table 1). This could be assumed that they were made from Al_2O_3 powder with different particle sizes. Also, the mole fraction of ZrO_2 to Al_2O_3 in Tool A ranked highest whereas those of Tool B and Tool C were almost 3 times less than that in Tool A. Thus, the superior efficiency in pinning mechanism in Tool A could be expected. Regardless to preparation techniques, it was predicted that Tool A might employ finer Al_2O_3 powder than Tool B and Tool C according to grain size measurement. Such fine particle size benefits the design of sintering schedule of the tool during manufacturing process in the way that high surface area of ultrafine powder enhances sintering ability. This led to relatively lower sintering temperature to get fully dense bodies and grain coarsening could be avoided. Along with relatively high ZrO_2 content, Al_2O_3 grains could not grow freely [13]. Meanwhile, larger Al_2O_3 particles took part in larger final grain size. It basically required higher sintering temperature to get fully dense bodies at the certain dwelling time and was prone to produce grain growth. With lower content of pinning particles, ZrO_2, pinning mechanism could not work very well.

After undergoing ultrasonic service, all used tools experienced slight grain coarsening but all grain sizes still retained their submicron levels. From micrographs illustrated in Figure 5, microstructural information was quantified and collected. It could be seen in Figure 6 that grain size distribution patterns of all tools were all in normal distribution manners, representing how scattered of Al_2O_3 and ZrO_2 grains in the selected areas of interest would be. Grain size distribution of Al_2O_3 and ZrO_2 in Tool A, however, had broader and the curves shifted to the right because of grain coarsening. Very slight shifts could be noticed for the distribution curves of Tool B and Tool C. Relationships between grain growth and ultrasonic energy at ambient temperatures have not yet been clearly stated. Grain coarsening in such fine grain structure might come from the ultrasonic energy exposure during service. Under continuous ultrasonic vibrational energy and stored energy along grain boundaries of fine grains, it possibly induced grain growth and also volume expansion from martensitic transformation of ZrO_2 from tetragonal to monoclinic. In the Al_2O_3-based bonding tools, The t-ZrO_2 which is partially stabilized form by the addition of yttria, is usually used in order that the t-ZrO_2 phase could change to monoclinic (m-ZrO_2) and improve toughness when stressed. In fact, Tool A should have retained microstructural changes like those of Tool B and Tool C. The noticeable coarsened Al_2O_3 and ZrO_2 grains might be occurred during thermal etching. Thermal etching carried out at 1500°C for 5 min was very common to reveal grain boundary in Al_2O_3-based composites. Such refined grains of Al_2O_3 were possibly sensitive to elevated temperature and this might relate to the tool thermal history. Tool A, denoted as the benchmark, provided superior properties including dense microstructure and toughness which was as a result of extra-fine grains and high ZrO_2 addition. Tool A was most likely to be sintered at lowest temperature than the others, so their grains after etching became coarser. Moreover, Tool A experienced longest ultrasonic cycles and reached 50k, meanwhile the other two did not yet overcome 50k. Such long ultrasonic cycles experience might attribute to the slight change in grain size than noticed in Tool B and Tool C.

Table 2. EDS area scans of the as-received tool samples.

Element	Tool A		Tool B		Tool C	
	Mass (%)	Atom (%)	Mass (%)	Atom (%)	Mass (%)	Atom (%)
O	37.40	64.06	34.28	51.44	24.61	39.86
Al	23.91	24.28	49.14	43.72	56.44	54.20
Zr	35.80	11.56	14.57	3.90	16.32	4.64
Cr	0.18	0.10	2.02	0.93	2.63	1.31

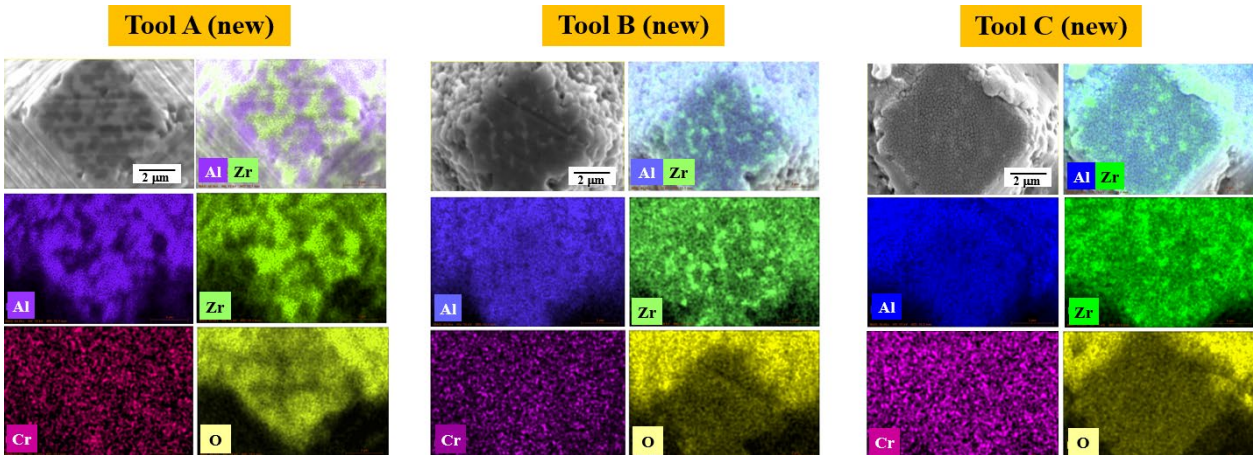

Figure 4. Mapping of the as-received tool samples.

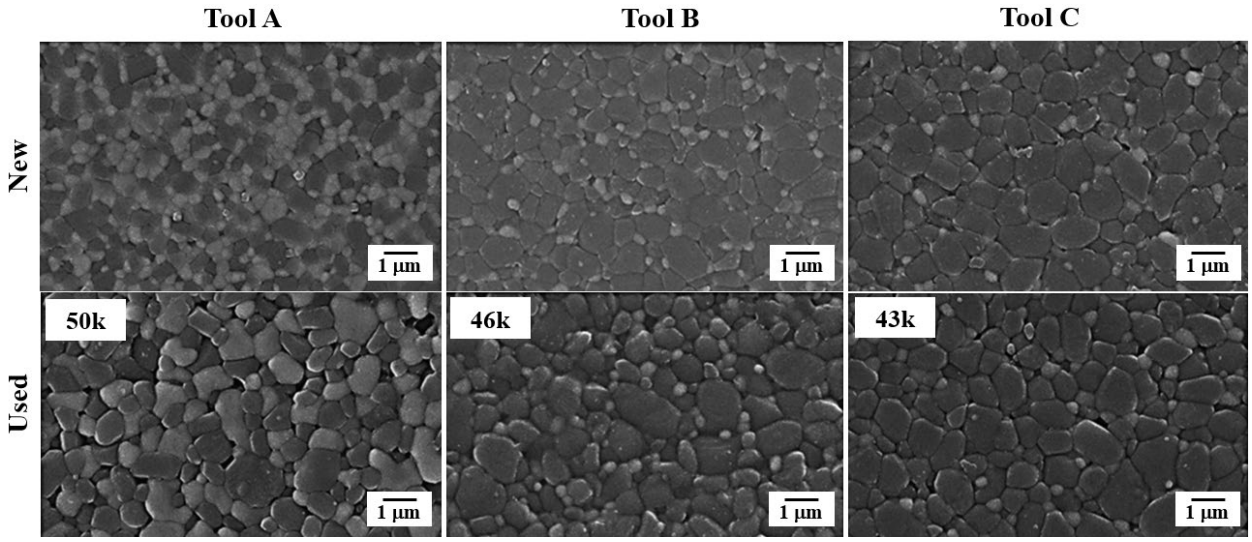

Figure 5. Backscattered electron micrographs of the tools before and after experiencing ultrasonic service up to 50k cycles.

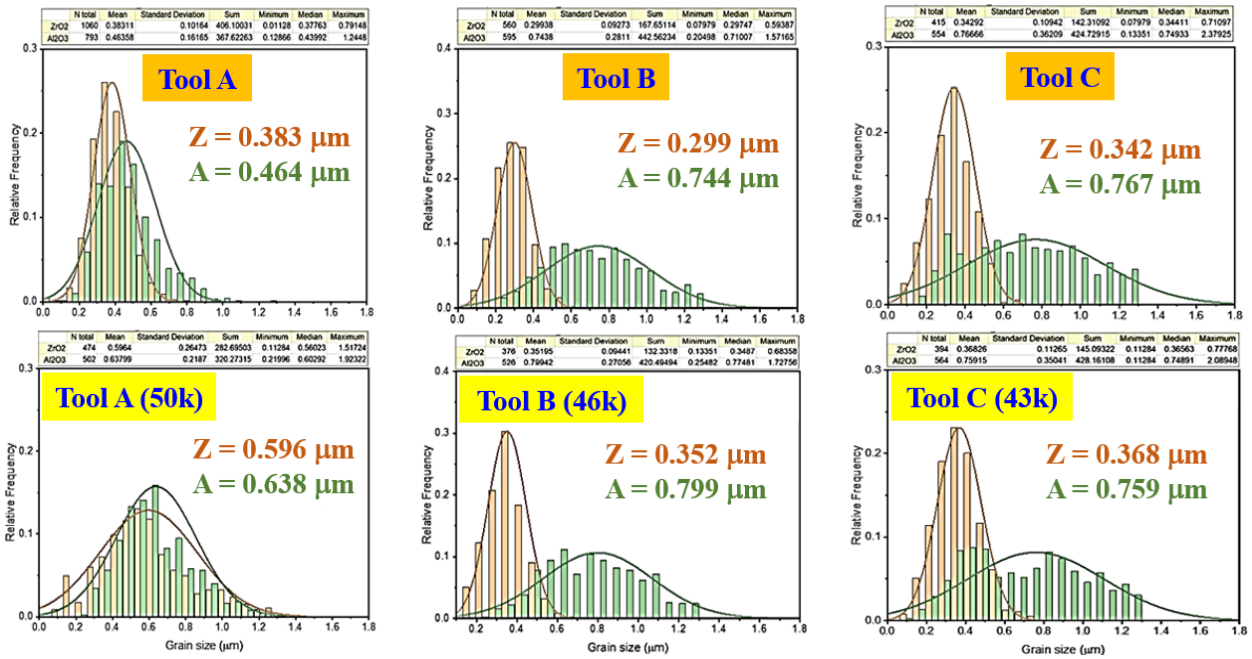

Figure 6. Grain size and grain size distribution of the tools before and after experiencing ultrasonic service up to 50k cycles

Density values of the three bonding tips are illustrated in Figure 7, showing that the density of Tool A ranked highest, followed by Tool C and Tool B, respectively. At the beginning, the samples were immerged in water until they were saturated before measuring the weight in water relative to that in the air. The obtained values were highly deviated because some air bubbles might trap at the waffle-end tip as well as in pores. Thus, the tip samples were de-aired while being immerged in water to remove the trapped air. It could be seen that even all tips are Al_2O_3-matrix reinforced with ZrO_2 and were claimed to be almost fully dense by the tool manufacturers, the density value of Tool B was lower than pure Al_2O_3. From the role of mixture (ROM), a mixture of Al_2O_3 and ZrO_2 like these tips is supposed to have the effective density value ranging between 3.98 $g{\cdot}cm^{-3}$ to 6.01 $g{\cdot}cm^{-3}$, assuming that the mixture are fully dense and no reactions between Al_2O_3 and ZrO_2 occurred. This suggested that Tool B micro-structure might contain a certain number of close pores compared to the others. SEM micrographs of the Tool B tips revealed that the diamonds located at the waffle-end was not very dense and porosity was also situated. In contrast, Tool A and Tool C were much well-arranged and much less defects and the density values of them agreed with the values declared in the manufacturer catalogs [1-3,9].

Vickers hardness testing of the bonding tools is conducted as shown in Figure 8. The results derived from Equation 1 suggested that hardness values almost unchanged according to the number of use (over 20k cycles). Unfortunately, the number of used Tool A at various cycles were too limited to examine the hardness values along the targeted service cycles, they all achieved targeted 50k. So, Tool A experimental data at various cycles was not included herein. This pointed out that ultrasonic energy had very slight effects on hardness even though it could slightly coarsen the grains. This agreed with the prediction of the hardness mentioned previously, Tool A had the lowest hardness value while those of Tool B and Tool C were in the same hardness levels. However, the values obtained from this investigation are lower than those mentioned by their manufacturers (around 2000 $kg{\cdot}mm^{-2}$ to 2200 $kg{\cdot}mm^{-2}$), as seen in Table 1. Used Tool B exhibited very slight decrease in hardness values, varying from the early cycles to almost targeted cycles (i.e. up to 50k). From the hardness results shown below, it could be noticed that the changes in hardness as a function of numbers of cycles were very small and could imply that the hardness values might not be very dependent to the number of cycles. This directly relates to the phase fraction and chemical composition of the tips.

With the same service, the fracture toughness were also obtained from the same sets of used Tool B and Tool C tips. Fracture toughness defines the ability of a material to resist the crack propagation or how a tool can absorb energy before it initiates a crack and reported in the term K_{IC}. This entity relates to microstructure and mechanical properties and can be calculated from various models, depending on crack type [16,18]. Fracture toughness of ceramics can be achieved by Vickers indentation technique, similar to hardness. Fracture toughness values are calculated from crack length propagated from the indented marks. There are two approaches to evaluate fracture toughness: (1) the calculation with Young's modulus and (2) the calculation without Young's modulus. The calculation of fracture toughness could be achieved by several models, the equations of which were stated in some literatures [e.g. 15]. It can be seen that the calculation models

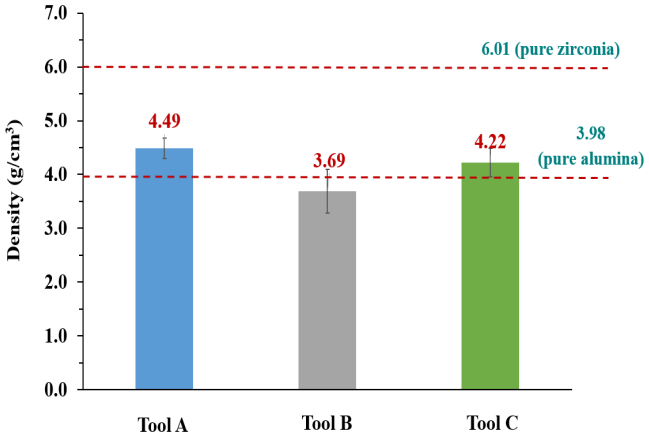

Figure 7. Measured density values of the tool samples.

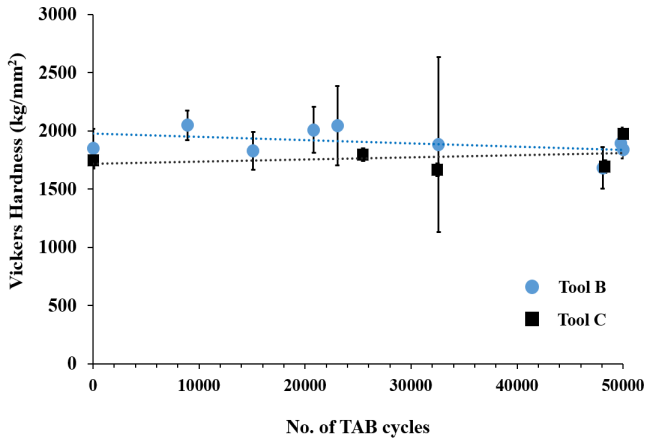

Figure 8. Variations in hardness of the tool samples from Vickers ndentation testing as a function of the numbers of TAB service.

also depend on the modes of crack types, either Palmqvist cracks or Median cracks. Palmqvist type always applies for the indentation with low applied load i.e. less than 50 N while the median one always applies for the indentation with load above 50 N. The bonding tools observed in this work used 10 kg or 98.1 N, thus it fell into Median crack type. This work relied on the Equation 2 proposed by Tanaka [14,15], the elastic modulus of which was neglected and the cracks presented in the tools fell into median type. The selected calculation model for K_{IC} from Vickers hardness introduced by Tanaka [14] therefore was more practical for this study because the actual elastic modulus could not be measured directly from such tiny tool samples. It was shown that the variation in the calculated fracture toughness values were also quite small similarly to that of the hardness values. Both used Tool B and Tool C tips provides the same levels of fracture toughness values and were independent from the number of TAB cycles, as shown in Figure 9. Since fracture toughness originates from Vickers hardness test, by measuring the size of the indented marks as well as the crack length, Figure 10 presents the crack length around the indented marks. The cracks of Tool A were relatively shorter that those of Tool B and Tool C, indicating that Tool A was comparatively tougher and could withstand crack propagation better than those of the others.

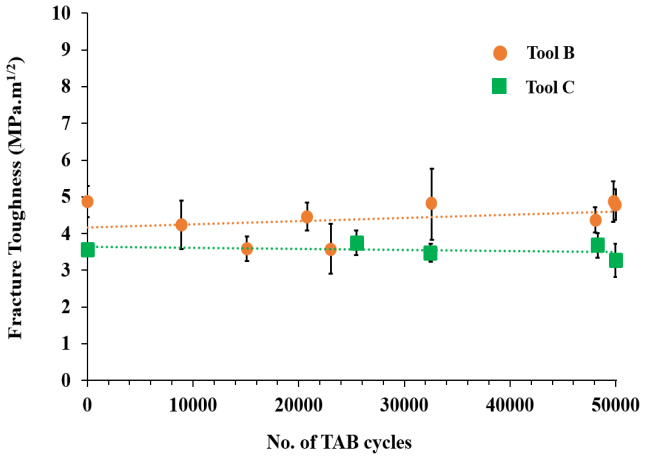

Figure 9. Variations in fracture toughness of the tool samples from Vickers indentation testing as a function of the numbers of TAB service.

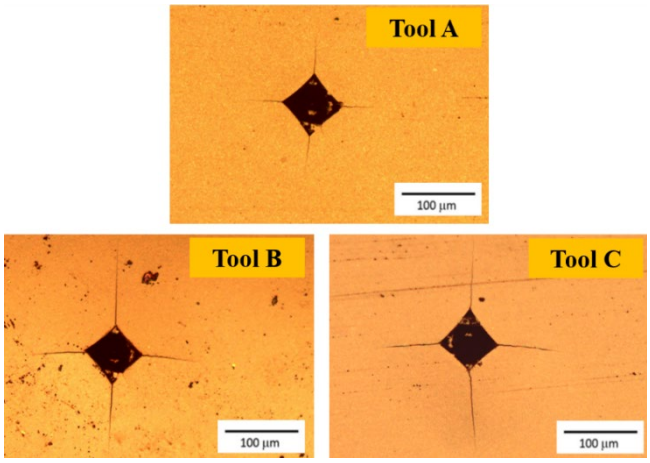

Figure 10. Cracks derived from Vickers indentation test of the new tool samples.

From the experimental data above, the numbers of TAB cycles did not affect physical properties of the bonding tools. These tools could sustain their hardness and fracture toughness even though their grain become slightly coarser. Hardness provides the ability to resist wear activities while fracture toughness reflected the ability to resist failure. However, it was seen from wear loss in Table 1 and Figure 2, showing the variation in wear loss among the three tools. With relatively similar bonding practice, the tool experiences the controlled ranges of applied load, power and elapsed TAB time [19]. A numerical study on ultrasonic factors of the head stack assembly reported that the bonding time of 325 ms to 425 ms had no effects on bonding process under the applied stress between 30 gf to 80 gf [20]. Under carefully controlled bonding parameters along with the low frequency, the elapsed time which the tool is stamped onto the coupling surface practically takes only approximately 10 ms to sustain production rate. A gradual increment of applied load and power is employed from a transducer to the bonding tip through a horn [4]. Also targeted at 50k cycles with qualified bonding performance, a combination of applied load and power increment is to be adjusted to achieve good bonding foot during service. According to the user, the increment rate of applied load and power is in a staircase pattern and might be manipulated during service to guarantee the quality of the bonding, but the ranges of applied load and power are still to be strictly controlled. Once the Tool A could not be afforded, Tool B and Tool C have come into candidates. Being set as the benchmark, the bonding parameters applied with Tool A was later employed to Tool B and Tool C. Disappointedly, the outcomes indicated that the Tool A's bonding parameters did not work well with Tool B and Tool C as expected. The candidate tools could not provide the same bonding performance and the lifetimes of them were not as last long as the benchmark one under the same service. This meant that the bonding parameters are specific for a tool and should not apply to other tools. So, the bonding parameters to work with Tool B and Tool B were to be adjusted. With several trial and error attempts, the user found that the increment rate of applied load and power in Tool B were higher when compared to that of Tool C. That led to different levels of damage in the form of worn surfaces among the tools.

The numbers of TAB cycles seemed strongly damaged the tip surface as seen from worn surfaces shown in Figure 2. However, the worse severely-worn surface could be noticed in Tool C at only 43k cycles compared with Tool A at 50k cycles and Tool B at 46k cycles. In fact, hardness and fracture toughness were likely to play their roles but Tool C which was harder than Tool A got more damaged, suggested by relative wear loss and surface profiles. Moreover, hardness and fracture toughness were insignificantly affected by the numbers of TAB cycles and might not be the main factors that confirm the quality of the bonding. This should involve bonding practice. Increased applied load could harm the tips by more intense rubbing with the coupled material during ultrasonic vibration. Meanwhile, increased power could provide higher intensity (amplitude) in order to get promising ultrasonic energy transfer through the medium. Ultrasonic energy transfer and bonding practice together with chemical composition and microstructural features of the tools might take part in the bonding quality and should be more focused.

Based on ultrasonic background and wave physics, the sound wave velocity travelling through an isotropic material depends strongly on microstructure and chemical composition. As mentioned in some literatures [e.g. 5,12,13], the ultrasonic velocity relates to elastic modulus and density of the tool material. The two entities depend on microstructures and chemical composition. Density itself could also be varied with the existence of flaws or defects, apart from phase fraction and phase composition. The tool with higher elastic modulus and density values could benefit ultrasonic velocity. From our experimental data, Tool A and Tool C yielded density values of 4.45 $g \cdot cm^{-3}$ and 4.22 $g \cdot cm^{-3}$, respectively, taking more than 90% of their theoretical density (TD) values calculated by ZrO_2 and Al_2O_3 fraction. In contrast, Tool B had lowest density, that is, only 85% of its TD. The flaw-containing structure at the tip of Tool B was confirmed by the electron micrographs (see Figure 1). From the chemical composition derived from the ICP-MS technique, Tool A was rich in ZrO_2 while the other two contain ZrO_2 in much lower contents. The tool with high content of ZrO_2 tended to offer greater mechanical strength and elastic modulus [11] also influenced by microstructure and grain size.

The characteristics of ultrasonic energy strongly depends strongly on the medium where the wave is travelling through [5]. A presence of discontinuity, like cracks, pores and flaws, along the wave path can reflect and refract the wave motion, then the information of defect site, orientation, size and other microstructural features can be collected. This is the core idea for the ultrasonic application by the mean of

ultrasonic velocity detection. Thus, the performance of the medium material to allow the wave to propagate is sensitive to the properties and microstructural features of the solid medium of interest. However, the medium material itself can impede the propagation of the travelling wave leading to less energy transfer, called acoustic impedance (Z). The role of this entity is not only to determine the acoustic transmission and reflection at the boundary of two different materials, but to allow the information to be collected during sound travelling through the medium. This benefits the ultrasonic transducer and service condition design. Normally, ultrasonic wave is reflected at the boundary or the interface between two different materials of which own its acoustic impedance, so called impedance mismatch, indicating the amount of incident wave energy reflects away from the targeted direction. To prevent reflection and to reduce the impedance across the boundaries due to air/material interfaces, the harder suppression of the bonding tool onto the bonding surface must be perfectly in contact. Furthermore, while the wave moves towards the medium, the amplitude of the wave can be weakened from scattering and absorption of the energy by the medium body. Scattering is the reflection of the sound in any directions, not in the original, expected directions of propagation. Absorption is the conversion of the sound energy to other forms of energy, like heat. The combination of scattering and absorption is so called attenuation, which is generally proportional to the sound frequency. Thus, the decay of the sound wave amplitude can be represented by the attenuation coefficient (α). The ultrasonic intensity or amplitude decrease exponentially due to either scattering or reflection, or both. As far the influences of microstructure on attenuation are considered, grain boundaries play their rules. At each grain boundary expresses discontinuity of elastic modulus, leading to the loss from random orientation in a polycrystalline solid. However, a fine-grain polycrystalline material is still preferred because fine grains tend to have lower attenuation compared with that of the coarser one at the same frequency. This can explained why Tool A is the most effective in ultrasonic energy transfer.

From the explanations above, Tool A provided several appropriate characteristics including fine-grain structures, high density and high ZrO_2 contents without a loss in hardness, thus good ultrasonic energy transfer was induced. Low applied force was employed and still offered good bonding ability with low wear loss. Tool C ranked second because of its high relative density values. It owned coarser grains and the wear loss was still high, however, the performance of Tool C was acceptable. Tool B the density values of which was low, required higher applied force to ensure high ultrasonic energy transfer. The highest Vickers hardness made Tool B have moderate wear loss, but it had poor strength. Practically, the user reckoned that most Tool B broke down during ultrasonic service or only few Tool B pieces could reach the targeted of 50k cycles with fair bonding performance.

4. Conclusions

The changes in microstructural features and physical properties as a result of ultrasonic service was determined and compared. All ceramic tool samples, Tool A, Tool B and Tool C were composed of $Al_2O_3$and ZrO_2 with different phase fractions. Their bonding performance depended on not only microstructural features but also bonding parameters. The number of ultrasonic cycles could give very slight changes in microstructural features and physical properties. It caused a modest grain growth in Al_2O_3-matrix structure while the size of ZrO_2 grains almost unchanged except in Tool A. Hardness and fracture toughness were not very sensitive to the number of TAB service. The deterioration of the tool surfaces in the form of wear involved ultrasonic bonding practice. Initial microstructural features of the tools affected ultrasonic energy transfer, thus the bonding parameters were to be adjusted. The application of force and power should be carefully and specifically designed.

Acknowledgements

The research team would like to thank Western Digital Storage Technologies (Thailand) Ltd. for full research funding and very kind cooperation. Thailand Institute of Scientific and Technological Research (TISTR) was appreciated for their helpful online service during COVID-19 shutdown. Thanks for Scientific and Technological Research Equipment (STREC) and Metallurgy and Materials Science Research Institute (MMRI) for the instrument service.

References

[1] Coorstek Inc., *Gaiser® precision bonding tools.* Product catalog, 2015.

[2] Small Precision Tools, *Bonding capillaries: Bonding evolution*. Product Catalog.

[3] Micro Point Pro, *TAB and magnetic head bonding tools*. Product Catalog.

[4] I. Lum, *Effects of ultrasound in microelectronic ultrasonic wire bonding*. PhD Thesis, Canada: University of Waterloo, Library and Archive Canada, Published Heritage Branch, 2007.

[5] D. K. Pandey, and S. Pandey, "18 - Ultrasonics: A technique of material characterization," *Acoustic Wave*, ed Dissanayake: Intech, 2010, pp. 298-430.

[6] S. F. Reiber, *Bonding tool.* Patent Application Publication, US2008/0197172A1 August 21, 2008.

[7] T. Nakano, *Ultrasonic bonding tool and ultrasonic bonding method.* Patent Application Publication, US10625475B2 April 21, 2020.

[8] W. J. Greig, "9 - Tape automated bonding - TAB," in *Integrated circuit packaging, assembly and interconnections*, Springer, 2007, pp.129-141.

[9] Small Precision Tools, *Gold and aluminum bonding wedge: bonding spectrum*. Product Catalog.

[10] H. Ma, and B. Zhao, "Prohibition effects on the crack propagation of Al_2O_3-ZrO_2 nano-composite ceramics under ultrasonic vibration," *Key Engineering Materials*, vol. 426-427, pp.147-150, 2010.

[11] M. Boniecki, T. Sadowski, P. Gołębiewski, H. Węglarz, A. Piątkowska, M. Romaniec, K. Krzyżak and K. Łosiewicz, "Mechanical properties of alumina/zirconia composites," *Ceramics International*, vol. 46, pp. 1033-1039, 2020.

[12] H. Carreon, A. Ruiz, A. Medina, G. Barrera, and J. Zarate, "Characterization of the alumina zirconia composite system by ultrasonic velocity measurements," *Materials Characterization,* vol. 60, no. 8, pp. 875-881, 2009.

[13] K. S. Tan, and P. Hing, "Ultrasonic through-transmission method of evaluating the modulus of elasticity of Al_2O_3–ZrO_2 composite," *Journal of Materials Science*, vol. 32, pp. 6633-6638, 1997.

[14] K. Tanaka, "Elastic/plastic indentation hardness and indentation fracture toughness: the inclusion core model," *Journal of Materials Science*, vol. 22, pp. 1501-1508, 1987.

[15] D. Ćorić, M. M. Renjo, and L. Ćurković, "Vickers indentation fracture toughness of Y-TZP dental ceramics," *International Journal of Refractory Metals and Hard Materials*, vol. 64, pp. 14-19, 2017.

[16] T. Ferreira, and W. Rasband, *ImageJ user guide IJ 1.46r*. Revised edition, 2004.

[17] Y. Yan, P. L. Xu, and B. Zhao, "Surface phase transformation analysis of nanozirconia toughened alumina ceramics under two-dimensional ultrasonic vibration grinding," *Applied Mechanics and Materials*, vol. 42, pp. 259-262, 2010.

[18] F. Sergejev, and M. Antonov, "Comparative study on indentation fracture toughness measurements of the cemented carbides," *Estonian Journal of Engineering*, vol. 12, no. 4, pp. 388-398, 2006.

[19] C. F. Luk, Y. C. Chan, and K. C. Hung, "Development of gold to gold interconnection flip chip bonding suspension assemblies," *Microelectron Reliability*, vol. 42, p. 3810389.

[20] J. Onpimai, and K. Tangchaichit, "A study on factors affecting the head stack assembly (HSA) in ultrasonic tab bonding process," *Khon Kaen University Research Journal*, vol. 16, no. 4, pp. 391-397, 2011.